Biological Rhythms Generated by a Single Activator-Repressor Loop with Inhomogeneity and Diffusion

Pablo Rojas,[1,*] Oreste Piro,[1,2,3] and Martin E. Garcia[1]
[1]Theoretical Physics and Center for Interdisciplinary Nanostructure Science and Technology (CINSaT), University of Kassel, Kassel, Germany
[2]Departament de Física, Universitat de les Illes Balears, Palma de Mallorca, Spain
[3]Institut Mediterrani d'Estudis Avançats, IMEDEA (CSIC–UIB), Esporles, Spain

(Received 21 March 2023; accepted 19 April 2024; published 27 June 2024)

Common models of circadian rhythms are typically constructed as compartmental reactions of well-mixed biochemicals, incorporating a negative-feedback loop consisting of several intermediate reaction steps essentially required to produce oscillations. Spatial transport of each reactant is often represented as an extra compartmental reaction step. Contrary to this traditional understanding, in this Letter we demonstrate that a single activation-repression biochemical reaction pair is sufficient to generate sustained oscillations if the sites of both reactions are spatially separated and molecular transport is mediated by diffusion. Our proposed scenario represents the simplest configuration in terms of the participating chemical reactions and offers a conceptual basis for understanding biological oscillations and inspiring *in vitro* assays aimed at constructing minimal clocks.

DOI: 10.1103/PhysRevLett.132.268401

Biological rhythms such as circadian, infradian and ultradian ones often originate in oscillations at a cellular level induced by complex mechanisms of gene auto-regulation composed by a number of coupled molecular reactions [1–4]. An activation-repression process alone leads to a single-mode dynamical system with negative feedback, which is unable by itself to support oscillatory behavior. Therefore, cellular clocks must resort to some form of delay mechanism that effectively complements the negative feedback naturally implicit in the repression component to achieve limit-cycle dynamics. Most common models of such cellular rhythms are based on compartmental descriptions (individual substances reacting in a homogeneous well-mixed batch) of the biochemistry, including several intermediate molecular reactions such as transcription, translation, phosphorylation, degradation, etc. Although the spatial inhomogeneities inside of the cell are recognized to play a role, and the transport of molecules between different regions of the cell should be taken into account, this is usually done by mimicking such transport as an extra compartmental reaction [1,5]. For example, messenger RNA (mRNA) migration from the nucleus is represented as "nuclear mRNA" reacting to produce "cytoplasmic mRNA" in the same hypothetical well mixed compartment. In order to oscillate, this kind of model needs to include at least three reaction steps in the loop, but often a much larger number is required to avoid unrealistic parametrization of the reaction constants [6]. The purpose of this Letter is to demonstrate that a much simpler reaction scheme is possible if the inhomogeneities of the reactants distributions and the transport are properly assessed. In particular, we will show only one step expression-repression negative-feedback reaction is enough to produce sustained circadian oscillations, provided that the locations of transcription and translation are spatially separated and molecular transport is mediated by intracellular diffusion.

In a well-mixed reaction model, a single expression-repression reaction step is commonly represented in an abstract manner by the following couple of ordinary differential equations [6,7]

$$\dot{M}(t) = \omega_M \frac{1}{1+P(t)^h} - \gamma_M M(t),$$
$$\dot{P}(t) = \omega_P M(t) - \gamma_P P(t). \quad (1)$$

$M(t)$ and $P(t)$, respectively, denote the time evolution of the concentrations of the mRNA—produced by a given gene—and of the protein—translated from the same mRNA—which repress the production of further mRNA. The inhibitory ability of P is governed by the Hill type function in the first term in the right hand side of the first equation, while the second term represents the spontaneous degradation process of mRNA at a rate γ_M. In turn, the rate of production of P is proportional to the concentration M,

while P degrades at a rate γ_P. The so-called *cooperativity* parameter h in the Hill function accounts for the number of molecules necessary to inhibit the expression of the corresponding gene. Notice that the divergence of the vector field defining this dynamics is constant and negative for any values of the pair (M, P). This means that the dynamical system contracts areas of any element of the state-space and therefore it cannot support limit cycles or self-sustained oscillations [6]. Instead, it can be proved that Eqs. (1) only have stable fixed points as stationary solutions.

In the context of compartmental models, hence, to generate a cellular rhythm with a biochemical circuit involving expression-repression feedback, it is imperative to incorporate an additional intermediate reaction. This reaction step is essential for introducing a delay capable of destabilizing one of the resting states. One such example, as proposed by Goodwin [7], is

$$\begin{aligned}\dot{M} &= \omega_M \frac{1}{1+R^h} - \gamma_M M,\\ \dot{P} &= \omega_P M - \gamma_P P,\\ \dot{R} &= \omega_R P - \gamma_R R,\end{aligned} \tag{2}$$

where P is an extra metabolite that mediates the production of the blocking protein R. This model does produce oscillations provided that $h > 8$, a value quite far from a realistic interpretation so that more sophisticated models resort to include a few extra steps of phosphorylation and dephosphorylation before the actual repression takes place [2]. An extension of Eqs. (2) to n reaction steps is straightforward (see Supplemental Material [8]), and schematically shown in Fig. 1(a). Figure 1(b) shows a plot of the minimal h that enables oscillations in a compartmental model of n components, as dictated by the so-called *secant* condition [14].

The real world, however, is neither compartmental nor well mixed. The cells are of small but finite size and inside them a great deal of inhomogeneity is present—localization

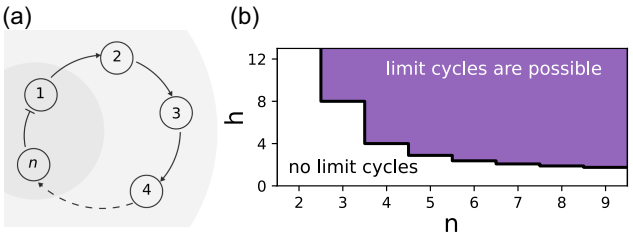

FIG. 1. (a) Scheme of the Goodwin model. A biochemical negative feedback loop where each component is produced by a first order reaction from the previous component, with the exception of the first one, whose zero-order reaction is repressed by the last component. (b) Secant condition. Minimal cooperativity that leads to oscillations for each length n of the biochemical chain.

of species occur within nanodomains [15–19]. While mRNA translation occurs in some place in the cytoplasm relatively distant from the nucleus, it is in this nucleus where the gene generates the mRNA and where the resulting protein may exert its repressive influence. Therefore, one trip of a new born mRNA molecule to the cytoplasm sites populated by ribosomes and another trip of the repressing proteins back to the nucleus are needed to complete the cycle of expression and repression. In the compartmental approach, this traffic is introduced in the form of fictitious intermediate reaction steps: $\mathrm{mRNA_{nucleus}} \to \mathrm{mRNA_{cytoplasm}}$, $\mathrm{P_{cytoplasm}} \to \mathrm{P_{nucleus}}$, etc., each one providing an equation of a similar structure as Eq. (2). A related and less realistic approach consists in introducing a prescribed delay in the equations [3,20], with the purpose of mimicking molecular transport times as well as extra steps.

In our study, in contrast, we investigate the impact of incorporating a realistic model for the transport across the inhomogeneities of the cell relying on the process of molecular diffusion. The outcome is startling: a loop containing the processes described in Eqs. (1) now exhibits oscillations. Furthermore, not only does it oscillate, but it also requires a cooperativity h much smaller than the simplest compartmental model capable of generating cellular rhythms.

Indeed, the investigation of the role of heterogeneity in the emergence of oscillations in reaction-diffusion systems, where the homogeneous counterpart exhibits only intrinsic homeostatic equilibrium, has a long history. For example, this role in the oscillatory behavior of pancreatic β cells has been thoroughly studied in [21]. More recently, several studies have examined various gene regulatory networks under the same framework [22–26]

In our model, as in real cells, the transcription and translation processes occur in spatially distinct regions. Specifically, the gene produces mRNA within the nucleus, which is well separated from the ribosomes where protein synthesis takes place. Both mRNA and protein migrate through diffusion, a process that causes both space and time dependence of the corresponding concentration distributions $m(\vec{r}, t)$ and $p(\vec{r}, t)$. Therefore, Eq. (1) reformulated to account for diffusion, results in

$$\begin{aligned}\dot{m}(\vec{r},t) &= \frac{\omega_m f_{\mathrm{GEN}}(\vec{r})}{1+p(\vec{r},t)^h} - \gamma_m m(\vec{r},t) + D_m \nabla^2 m(\vec{r},t),\\ \dot{p}(\vec{r},t) &= \omega_p f_{\mathrm{RIB}}(\vec{r}) m(\vec{r},t) - \gamma_p p(\vec{r},t) + D_p \nabla^2 p(\vec{r},t),\end{aligned} \tag{3}$$

where $f_{\mathrm{GEN}}(\vec{r})$ and $f_{\mathrm{RIB}}(\vec{r})$ are the spatial distributions of the gene and the ribosomes, respectively. D_m and D_p are the effective diffusion coefficients experienced by the mRNA and P molecules. The parameters ω_m and ω_p are the rates of production of mRNA and P. Eqs. (3) reduce to the Goodwin model for two components if one neglects the

dependence of the concentrations on the spatial coordinates (well-mixed regime).

Of course, Eqs. (3) can be generalized to include also intermediate reactions, but we start by focusing on the simpler case, equivalent to the nonoscillatory $n = 2$ member of the Goodwin family [7]. Let us also begin by considering the spatially one-dimensional (1D) version of Eqs. (3), obtained after the replacements $\vec{r} \to x$ and $\nabla^2 \to \partial_{xx}$, within the spatial domain $\Omega = [-R_{\text{cell}}, R_{\text{cell}}]$, with impermeable (zero flux) boundary conditions. As a preparatory analysis, we also set the diffusion and degradation parameters as $D_m = D_p = D$ and $\gamma_m = \gamma_p = \gamma$. Finally, we choose the corresponding distributions $f_{\text{GEN}}(x)$ and $f_{\text{RIB}}(x)$ to be boxcar functions centered around the positions $x_m = 0$ and $x_p \neq 0$ and of corresponding widths $2R_m$ and $2R_p$, respectively. x_p is measured in units of the characteristic length $\lambda = \sqrt{D/\gamma}$ (see the model details in Supplemental Material [8]).

For comparison with the compartmental models, we compute the integrated quantities $M(t) = \int_\Omega m(x,t)dx$ and $P(t) = \int_\Omega p(x,t)dx$ from the simulated $m(x,t)$ and $p(x,t)$. These quantities are comparable to the corresponding concentrations of the Goodwin's family.

Figure 2(b) presents a parametric plot of $M(t)$ and $P(t)$ evolving from two different uniform initial configurations $m(x,0) = m_{0i}$, $p(x,0) = p_{0i}$, $i = 1, 2$, corresponding to initial bulk quantities (M_1, P_1) and (M_2, P_2), respectively. The inter-reaction-sites distance has been set to $x_p = 3$ and the cooperativity to $h = 4$. The asymptotic convergence to a limit cycle is evident, confirming the existence of stable oscillations in the system and suggesting a certain correspondence with a compartmental model with at least three reaction components. However, the compartmental modeling approach necessitates a much longer loop to produce oscillations with the same level of cooperativity as our model. In fact, Fig. 2(c) illustrates the onset of oscillations as h is varied from small values, where no limit cycles are observed, to larger values where oscillations emerge. The bifurcation occurs at $h \lesssim 3$, which in the compartmental model would require a loop of six reactions ($n = 6$, see Fig. 1). The oscillations observed in our $n = 2$ model arise from the delays induced by the diffusive transport of the chemical species. The timescale of these delays can be estimated from the analytical expression of the spatial Green function of the degradation-diffusion equation, resulting in the *relaxation time* $t_R = (1/4\gamma)[\sqrt{1 + 4(x/\lambda)^2} - 1]$. t_R becomes asymptotically linearly dependent on the distance, a behavior that reflects proportionally on the period of the oscillations, as well as the slopes of the patterns in the spatiotemporal distribution of $m(x,t)$ and $p(x,t)$ shown in Supplemental Material [8], Fig. S9.

The series of 3D plots in Fig. 2(d), illustrates the evolution of the asymptotic dynamics of $M(t)$ and $P(t)$

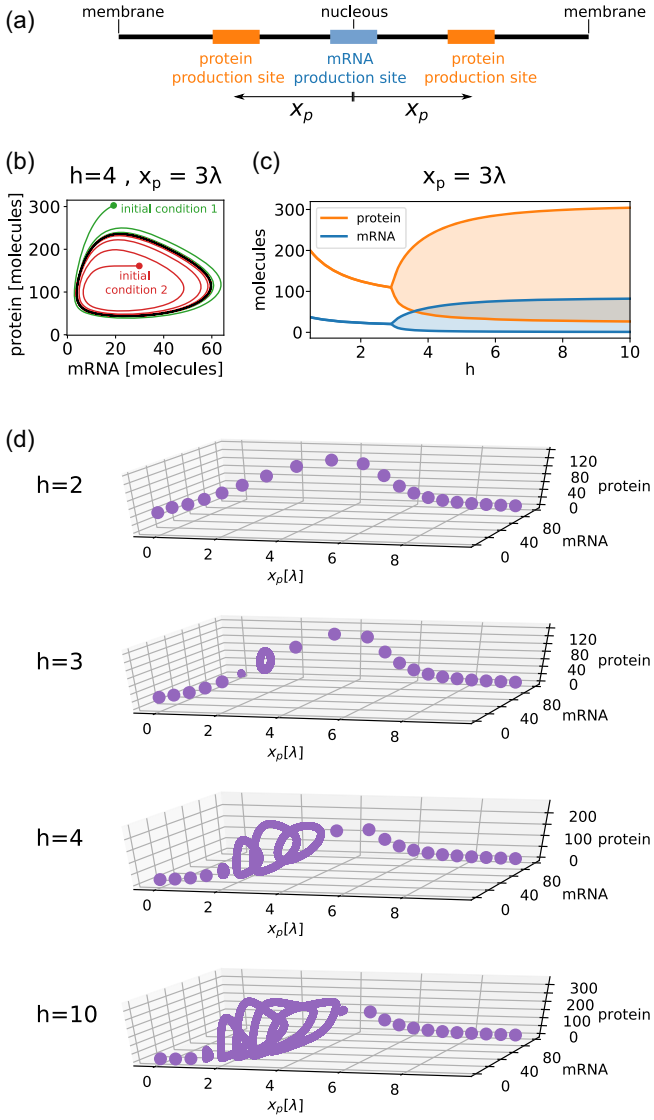

FIG. 2. (a) Scheme of the 1D model with zero flux boundary condition at the membrane [Eq. (3)]. (b) Parametric plot in terms of the bulk quantities of mRNA and protein, $M(t)$ and $P(t)$, showing two example trajectories (red, green) converging to the limit cycle (black) for $h = 4$. (c) Plot of minima and maxima (lines) as a function of h, with shaded regions indicating oscillations, which occur below $h = 3$. (d) Trajectories after initial transient of the quantities $M(t)$ and $P(t)$ for different distances and cooperativities. The higher the cooperativity h, the wider the range of distances where oscillations occur, up to the interval $[2\lambda, 4\lambda]$ for $h = 10$. The case $h = 3$ shows oscillations for a narrow range of distances. $D = 0.1$, $\gamma = 0.1$, $R_m = R_p = 0.5$, $R_{\text{cell}} = 10$, $\omega_m = 10$, $\omega_p = 20$.

as a function of x_p for several values of h. For both small and large distances x_p, the dynamics settle in fixed points. For small x_p, such behavior aligns with that of the two-component well-mixed Goodwin model where oscillations are absent. The death of the oscillations at large distances (i.e., long delays) is instead due to the degradation of P

before reaching the nucleus, leading to a deficiency in protein to repress mRNA production. An estimation of the upper limit of available proteins at the gene is provided in Supplemental Material [8]. Remarkably, for intermediate nucleus-ribosomes distances, the system exhibits sustained oscillations. It is also worth noting that with increasing cooperativity, the range of x_p values conducive to oscillations widens, and the minimum required value to induce oscillations decreases. Even with the modest cooperativity level of $h = 3$, our model exhibits limit cycles across a significant range of nucleus-ribosome distances. This finding underscores the significance of purely diffusive transport in enabling oscillatory behavior within a negatively feedback-controlled circuit involving only two species.

The emergence of self-sustained oscillations in this scenario is not an artifact of the partial differential equations (PDE) representation. We have confirmed their existence by running simulations of an agent-based stochastic counterpart of the deterministic PDE. In this alternative scheme, diffusion of individual molecules throughout the spatial domain is represented by a Langevin equation, while creation and degradation of molecules is simulated via a Gillespie algorithm. Molecules are therefore subjected to the following set of transitions

$$\begin{aligned} &\text{mRNA} \to \phi; \qquad \phi \to \text{mRNA} \\ &\text{protein} \to \phi; \qquad \phi \to \text{protein} \\ &x_i(t + \Delta t) = x_i(t) + \sqrt{2D\Delta t}\xi \end{aligned} \tag{4}$$

whereby ϕ denotes fictitious dynamically irrelevant chemical species representing the residues of degradation and the source of synthesis of both mRNA and protein molecules, $x_i(t)$ is the position of the molecule i at time t and ξ is a Gaussian white noise [27]. Each reaction rate is set equivalent to Eq. (3) (see in Supplemental Material [8]). D is the diffusion coefficient common to both species. Figure 3(a) shows a comparison between the simulations of the 1D deterministic and stochastic versions. Notice that both display oscillations of similar periods for distances x_p within the same ranges.

In a similar vein, we have confirmed that the emergence of oscillations through this mechanism also occurs in higher spatial dimensions [Fig. 3(b) and Supplemental Material [8]]. For illustration we show in Fig. 3(b) the results of simulations conducted with the stochastic version for a two-dimensional (2D) circular cell, where the ribosomes are randomly distributed within annular regions of different inner radii $r_{\min}$ and an outer radius R_{cell} (the radius of the cell). The nucleus is positioned at the center of the cell. The qualitative agreement with the behavior observed in the 1D versions is evident: oscillations also manifest for intermediate values of the minimal distance $r_{\min}$ between the nucleus and the ribosomes, while disappearing for both small and large values of $r_{\min}$. A detailed comparison between 1D and 2D models for both the deterministic and stochastic settings is included in Supplemental Material [8].

To explore the impact of diffusion in more complex reaction schemes we studied the loop with three molecular species of Eqs. (2) including now segregation and

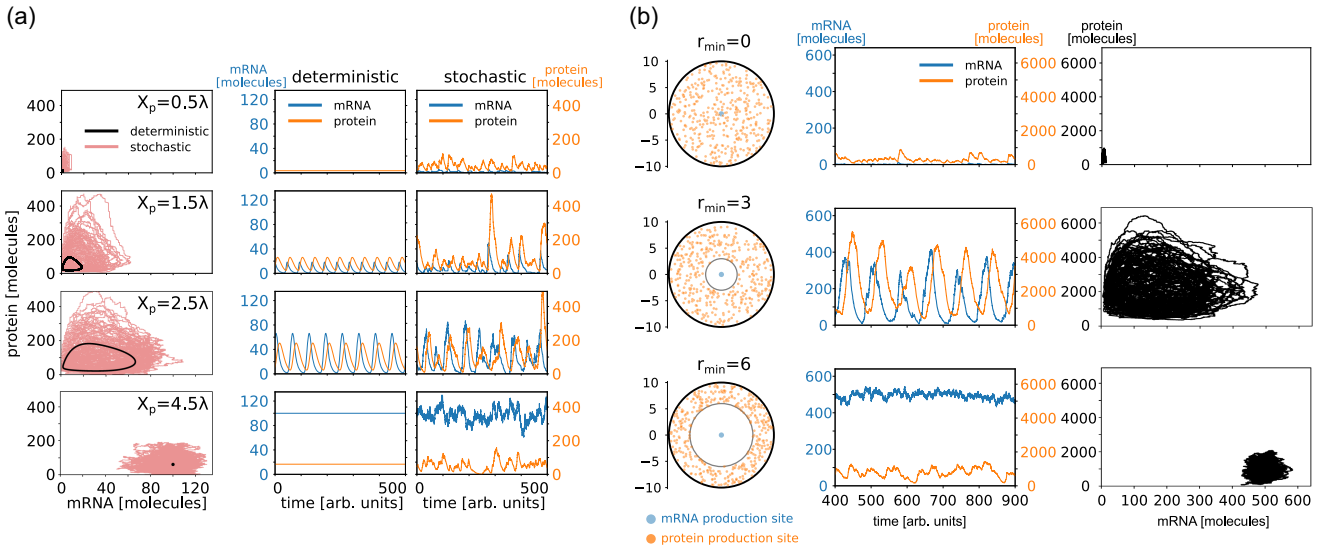

FIG. 3. (a) Stochastic (agent-based) and deterministic (PDE) representations show the onset of oscillations of the number of mRNA and protein molecules in approximately the same range of separations. Left panel column: superimposed trajectories from the deterministic and stochastic models. Middle and right columns: time series of mRNA and protein in a segment of the same trajectories. $h = 10$, $D = 0.1$, $\gamma = 0.1$, $R_m = R_p = 0.5$, $R_{\text{cell}} = 10$, $\omega_m = \omega_p = 10$ (b) Stochastic agent-based model in 2D, with minimal distance $r_{\min}$ for the randomly localized protein production sites. The number of molecules fluctuates with no oscillations for small and large distances, and oscillates for intermediate distances. See Supplemental Material [8] for model details.

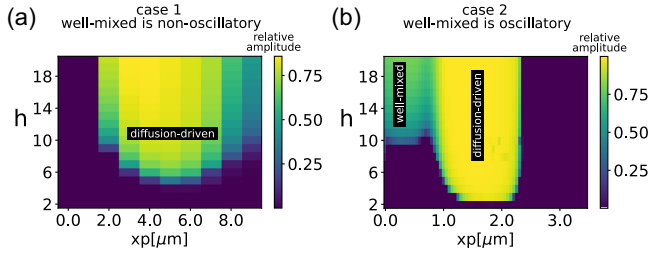

FIG. 4. Enhanced oscillations emerge in example biochemical loops of three species when sources of molecular species are spatially separated: (a) A fictitious feedback loop of three species compatible with experiments [15,28] that would not oscillate in the well-mixed case, displays oscillations if the distance between sources is appropriate. (b) A feedback loop that oscillates in the well-mixed case [29], exhibits reduced or disappearing oscillations as sources are separated, followed by rebounded oscillations upon increasing distance ($x_p \simeq 0.7$ μm, $h = 8$–10).

diffusion. We have chosen two parameter sets. In one, both kinetic and transport parameters are compatible with experimental measurements on biological systems [15,28]. In the second set, kinetic parameters are taken from published compartmental models that display oscillations in the well-mixed scenario [29] (see complete parameter list in Supplemental Material [8]). The production site distributions are set to be the same for both the P and R species ($x_r \equiv x_p$, $R_r \equiv R_p$). Figure 4 displays in color code the regions in the x_p-h plane where oscillations appear. The results for the first parameter set [Fig. 4(a)] demonstrate that a simple negative feedback loop in a biological cell can transition from static to oscillatory behavior for distances compatible with the dimensions of a cell, provided the cooperativity is at least 5. The results from the second set [Fig. 4(b)] highlight a significant observation: oscillations of a system prepared to oscillate in the absence of spatial separation (well mixed) may weaken as the distance between sources starts to increase [upper-left corner of panel (b), in the region around $x_p \simeq 0.7$ μm] up to an extent where they eventually disappear ($h = 8$–10). Interestingly, these oscillations rebound with greater amplitude as the separation distance is further extended (diffusion driven), see Fig. S10 in Supplemental Material [8] for more details. Moreover, diffusion-driven oscillations manifest over a broader parameter range, requiring much smaller values of h compared to the well-mixed condition. The distinct characteristics of these two oscillatory regions, including their shapes and amplitudes, suggest that diffusion not only serves as a unique mechanism for inducing oscillations but also enhances their robustness.

Finally, we want to stress that our results are robust against the removal of simplifying assumptions of the former description such as symmetries, coefficients uniformity, etc. For instance, we have tested the persistence of the scenario in the presence of nonuniform diffusion coefficients mimicking the complexity of the crowded intracellular environment. We observed only moderate quantitative changes to the same qualitative features of the oscillatory regime (Fig. S7 in Supplemental Material [8]). Moreover, the scenario remained also robust when the location and number of ribosomes were made arbitrary. Both 1D and 2D deterministic and stochastic numerical simulations confirmed that symmetric and nonsymmetric ribosome distributions of various sizes, situated at different locations, and within cells of varying diameters, exhibit oscillations across an appropriate range of nucleus-ribosome distances (see Supplemental Material [8] Figs. S3–S6). Interestingly, ribosomes located closer to the nucleus turn out to exert a dominant influence on the onset of oscillations, due to the shorter delays they induce (see Figs. S3 and S4 in Supplemental Material [8]).

Summarizing, we have shown that a simple biochemical feedback loop, that in well-mixed conditions would be doomed to display static behavior, can be turned into an oscillator by physically separating the domains where reactions occur. This study can reconcile the parameter choice in mathematical modeling with the biologically plausible values. It can provide the modeling framework to recent experimental observations that suggest a crucial role of the localization of synthesis within cells [15–18,30]. Furthermore, the scope of the results presented here can find direct applications in the field of synthetic biology, in which the dynamics of cell-like compartments can be tuned via its geometry to display oscillations [31].

We thank Claudia R. Arbeitman for useful discussions. This work has been supported by the Deutsche Forschungsgemeinschaft through the Grant No. RTG 2749/1 "Biological Clocks on Multiple Time Scales." M. E. G. and P. R. acknowledge University of Kassel through ZFF-PROJEKT 2377 and the Graduate Program Biological Clocks. O. P. acknowledges COST Action CA21169, the MICIN Mobility Contract No. PRX22/00522, and the Maria de Maeztu Grant No. CEX2021-001198-M funded by MCIN/AEI. P. R. acknowledges support from the Joachim Herz Foundation.

*Corresponding author: pablo.rojas@uni-kassel.de

[1] D. B. Forger, *Biological Clocks, Rhythms, and Oscillations: The Theory of Biological Timekeeping* (MIT Press, Cambridge, MA, 2017).
[2] D. Gonze, J. Halloy, and A. Goldbeter, Deterministic versus stochastic models for circadian rhythms, J. Biol. Phys. **28**, 637 (2002).
[3] B. Novák and J. J. Tyson, Design principles of biochemical oscillators, Nat. Rev. Mol. Cell Biol. **9**, 981 (2008).
[4] B. Ananthasubramaniam and H. Herzel, Positive feedback promotes oscillations in negative feedback loops, PLoS One **9**, e104761 (2014).
[5] A. Goldbeter, A model for circadian oscillations in the Drosophila period protein (PER), Proc. R. Soc. B **261**, 319 (1995).

[6] J. S. Griffith, Mathematics of cellular control processes I. Negative feedback to one gene, J. Theor. Biol. **20**, 202 (1968).
[7] B. C. Goodwin, Oscillatory behavior in enzymatic control processes, Adv. Enzyme Regul. **3**, 425 (1965).
[8] See Supplemental Material at http://link.aps.org/supplemental/10.1103/PhysRevLett.132.268401 for additional details on the model and numerical simulations, and derivation of relaxation times, which includes Refs. [9–13].
[9] A. M. Berezhkovskii, C. Sample, and S. Y. Shvartsman, Formation of morphogen gradients: Local accumulation time, Phys. Rev. E **83**, 051906 (2011).
[10] A. J. Ellery, M. J. Simpson, S. W. McCue, and R. E. Baker, Critical time scales for advection-diffusion-reaction processes, Phys. Rev. E **85**, 041135 (2012).
[11] M. Levy, R. Falkovich, S. S. Daube, and R. H. Bar-Ziv, Autonomous synthesis and assembly of a ribosomal subunit on a chip, Sci. Adv. **6**, eaaz6020 (2020).
[12] A. M. Tayar, E. Karzbrun, V. Noireaux, and R. H. Bar-Ziv, Propagating gene expression fronts in a one-dimensional coupled system of artificial cells, Nat. Phys. **11**, 1037 (2015).
[13] A. M. Tayar, E. Karzbrun, V. Noireaux, and R. H. Bar-Ziv, Synchrony and pattern formation of coupled genetic oscillators on a chip of artificial cells, Proc. Natl. Acad. Sci. U.S.A. **114**, 11609 (2017).
[14] J. J. Tyson and H. G. Othmer, The dynamics of feedback control circuits in biochemical pathways, Prog. Theor. Biol. **5**, 1 (1978).
[15] Y. Fonkeu, N. Kraynyukova, A.-S. Hafner, L. Kochen, F. Sartori, E. M. Schuman, and T. Tchumatchenko, How mRNA localization and protein synthesis sites influence dendritic protein distribution and dynamics, Neuron **103**, 1109 (2019).
[16] A.-S. Hafner, P. G. Donlin-Asp, B. Leitch, E. Herzog, and E. M. Schuman, Local protein synthesis is a ubiquitous feature of neuronal pre- and postsynaptic compartments, Science **364**, eaau3644 (2019).
[17] C. Sun, A. Nold, C. M. Fusco, V. Rangaraju, T. Tchumatchenko, M. Heilemann, and E. M. Schuman, The prevalence and specificity of local protein synthesis during neuronal synaptic plasticity, Sci. Adv. **7**, eabj0790 (2021).
[18] B. Wu, C. Eliscovich, Y. J. Yoon, and R. H. Singer, Translation dynamics of single mRNAs in live cells and neurons, Science **352**, 1430 (2016).
[19] P. K. Jackson, cAMP signaling in nanodomains, Cell **182**, 1379 (2020).
[20] G. Bordyugov, P. O. Westermark, A. Korenčič, S. Bernard, and H. Herzel, Mathematical modeling in chronobiology, in *Circadian Clocks*, edited by A. Kramer and M. Merrow (Springer, New York, 2013), pp. 335–357, 10.1007/978-3-642-25950-0_14.
[21] J. H. E. Cartwright, Emergent global oscillations in heterogeneous excitable media: The example of pancreatic β cells, Phys. Rev. E **62**, 1149 (2000).
[22] A. L. Krause, V. Klika, T. E. Woolley, and E. A. Gaffney, Heterogeneity induces spatiotemporal oscillations in reaction-diffusion systems, Phys. Rev. E **97**, 052206 (2018).
[23] F. Naqib, T. Quail, L. Musa, H. Vulpe, J. Nadeau, J. Lei, and L. Glass, Tunable oscillations and chaotic dynamics in systems with localized synthesis, Phys. Rev. E **85**, 046210 (2012).
[24] M. Chaplain, M. Ptashnyk, and M. Sturrock, Hopf bifurcation in a gene regulatory network model: Molecular movement causes oscillations, Math. Models Methods Appl. Sci. **25**, 1179 (2015).
[25] C. K. Macnamara and M. A. Chaplain, Diffusion driven oscillations in gene regulatory networks, J. Theor. Biol. **407**, 51 (2016).
[26] C. K. Macnamara and M. A. Chaplain, Spatio-temporal models of synthetic genetic oscillators, Math. Biosci. Eng. **14**, 249 (2017).
[27] R. Erban and S. J. Chapman, *Stochastic Modelling of Reaction–Diffusion Processes* (Cambridge University Press, Cambridge, England, 2020).
[28] M. Sturrock, A. J. Terry, D. P. Xirodimas, A. M. Thompson, and M. A. Chaplain, Spatio-temporal modelling of the Hes1 and p53-Mdm2 intracellular signalling pathways, J. Theor. Biol. **273**, 15 (2011).
[29] D. Gonze and W. Abou-Jaoudé, The Goodwin model: Behind the Hill function, PLoS One **8**, e69573 (2013).
[30] M. Weitz, J. Kim, K. Kapsner, E. Winfree, E. Franco, and F. C. Simmel, Diversity in the dynamical behavior of a compartmentalized programmable biochemical oscillator, Nat. Chem. **6**, 295 (2014).
[31] E. Karzbrun, A. M. Tayar, V. Noireaux, and R. H. Bar-Ziv, Programmable on-chip DNA compartments as artificial cells, Science **345**, 829 (2014).